Transient elasticity and the rheology of polymeric fluids with large amplitude deformations

Oliver Müller,[1] Mario Liu,[1] Harald Pleiner,[2] and Helmut R. Brand[2,3]
[1]*Institut für Theoretische Physik, Universität Tübingen, 72076 Tübingen, Germany*
[2]*Max Planck Institute for Polymer Research, 55021 Mainz, Germany*
[3]*Department of Physics, University of Bayreuth, 95440 Bayreuth, Germany*
(Received 10 July 2015; published 23 February 2016)

Transient elasticity is a systematic generalization of viscoelasticity. Its purpose is to give a coherent description of non-Newtonian effects displayed by soft-matter systems, especially polymer melts and solutions. Using the concept of transient elasticity we describe here a hydrodynamic model for polymeric fluids, which is applicable for large amplitude deformations. We present an energy density with only two independent parameters, which is compatible with all thermodynamic requirements and which reduces for small deformations to models studied previously. The expression discussed is simple enough to allow full analytic treatment and shows semiquantitative agreement with experimental data. This model is used to capture many of the interesting effects thought to be characteristic of polymer rheology for large deformations including viscosity overshoot near the onset of shear flow, the onset of elongational flows in situations for which there is no stationary solution as well as shear thinning and normal stress differences for a large range of shear rates. In addition, we analyze how well our model accounts for empirical relations including the Cox-Merz rule, the Yamamoto relation, and Gleißle's mirror relations.

DOI: 10.1103/PhysRevE.93.023114

I. INTRODUCTION

In the companion paper to this one [1] [referred to as part (I) here] we used a strong simplification of the hydrodynamic model for polymeric fluids to describe a number of simple flows. The most important assumptions used were the restriction of the expansion of the energy density in powers of the Eulerian strain tensor, U_{ij}, to fourth order and the simplifcation of its dynamic equation by assuming a single relaxation behavior and neglecting a dissipative cross-coupling to extensional flow. The resulting simplified model is therefore only valid in the limit of small strains and contains in total five parameters, namely, the relaxation time, τ, of the transient network, the three elastic constants K_1, K_2, and K_3 associated with quadratic, cubic, and quartic transient elasticity and the viscosity parameter η_∞. It turned out that for low shear and elongation rates the predictions of the model agree well with experimental observations. It is, for example, possible to capture the onset of shear thinning for a stationary shear flow, surface effects including the Weissenberg effect [2–5], and the surface curvature for the flow down a slightly tilted channel [6]. In addition, one can make predictions about the elongation rate dependence of the Trouton viscosity.

There is, however, a range of other fundamental and interesting effects, which only arise for larger deformations. These include the viscosity overshoot for the onset of shear flow as well as the onset of elongational flow in situations in which the elongation is so large that a stationary state no longer exists. It also appears to be desirable to investigate shear thinning for a large range of shear rates and to analyze the two normal stress differences as a function of shear rate. The key challenge is to generalize model (I) [1] to large deformations without losing the useful results obtained so far in the limit of small strains, but still maintaining the simplicity and universality of the description.

One possibility would be to extend the nonlinear dynamic equations for U_{ij}. However, the version used in part (I) [1], with a single linear relaxation term, has the advantage that one can get a solution for the strain tensor without the need to know the explicit structure of the energy. We want to still benefit from this property and, thus, leave unchanged the dynamic equation for the strain tensor,

$$\dot{U}^0_{ij} + v_k \nabla_k U^0_{ij} - A_{ij} + [U_{kj}\nabla_i v_k + U_{ik}\nabla_j v_k]_0 = -\frac{1}{\tau} U^0_{ij}, \tag{1}$$

where the superscript 0 refers to the traceless part and $A_{ij} = A^0_{ij}$ because of the assumed incompressibility.

Instead, we focus on the generalization of the energy density. An obvious step in this direction would be a generalization of the energy expansion beyond the fourth order in U_{ij}. An expansion to higher orders, however, has the disadvantage of generating a larger number of elastic parameters that are difficult to determine. Therefore we use a different route that is a simple extension into the nonlinear deformation domain. Based on general considerations we design in Sec. III an energy density that is used in the subsequent sections to discuss the flow behavior for large amplitude deformations. In Sec. IV stationary and relaxing (as well as the onset of) shear flows with large strains are considered. Elongational flows with large deformations are discussed in Sec. V. In addition, in Sec. VI we analyze how well we can capture empirical relations that relate different material functions to different kinds of flow. In particular, we discuss the Cox-Merz rule [7], the Gleißle mirror relations [2,8], the Laun rule [2,9], and the Yamamoto relation [10,11]. Finally, some conclusions and a perspective are given in Sec. VII.

First, however, in the next section (II) we discuss what can be learned about the stress tensor from the general properties of the energy without using an explicit expression for it. This sets the framework for some stress-strain relations and guides the development of the energy density we choose to deal with large amplitude flows.

 ©2016 American Physical Society

II. GENERAL PROPERTIES OF THE ENERGY AND THE STRESS TENSOR

To address large deformations it is necessary to generalize the energy density in a way so that the corresponding expression is not valid just for small deformations. So far a general expression for the energy density for large deformations is unknown. Therefore we investigate first what general conclusions can be drawn from thermodynamic arguments and we construct an energy density qualitatively satisfying these constraints. For this construction we draw on existing work on nonlinear deformations of elastic solids (compare Refs. [12] and [13] for an overview of the field of rubber elasticity).

For a general treatment we first recall the approach for small deformations. In the rest frame we assumed that we can use the energy density $\varepsilon^{\rm rf}$ as a starting point and that the parts depending on the entropy and mass density can be separated from the elastic contributions:

$$\varepsilon^{\rm rf}(s,\rho,U_{ij}) = \bar{\varepsilon}(s,\rho) + \varepsilon^{\rm ela}(U_{ij}). \tag{2}$$

In the following we want not to expand $\varepsilon^{\rm ela}$ but, rather, to analyze what properties this energy density possesses and how one can represent it simply. As mentioned in [1], the elastic energy density can only be a function of the three invariants of U_{ij}. In order to be able to make comparisons with the usual representations of the nonlinear elasticity [12–14], we do not use $\mathrm{Tr}(\mathbf{U})$, $\mathrm{Tr}(\mathbf{U}^2)$, and $\mathrm{Tr}(\mathbf{U}^3)$ but, rather, the three stretch coefficients λ_1, λ_2, and λ_3. The latter describe the relative distortions along the principal axes of the strain tensor for a given type of flow. We therefore rewrite Eq. (2) as

$$\varepsilon^{\rm rf} = \bar{\varepsilon}(s,\rho) + \varepsilon^{\rm ela}(\lambda_1,\lambda_2,\lambda_3). \tag{3}$$

Next we analyze which general statements are possible about $\varepsilon^{\rm ela}$. Since we focus here on isotropic systems, $\varepsilon^{\rm ela}$ must reflect this symmetry as well. This means explicitly that an interchange of λ_i and λ_j with $i \neq j$ in $\varepsilon^{\rm ela}$ cannot change the structure of the energy density. All properties which the energy density has regarding λ_1 must also apply to λ_2 and λ_3. In addition, it is clear intuitively that the elastic energy in the undeformed state must have a global minimum for $\lambda_1 = \lambda_2 = \lambda_3 = 1$. In the following we set the energy for this global minimum to $\varepsilon^{\rm ela} = 0$. For arbitrary deformations we therefore always have $\varepsilon^{\rm ela} > 0$. If the system is, on the other hand, infinitely strongly stretched or compressed, then the elastic energy will diverge:

$$\lim_{\lambda_i\to\infty} \varepsilon^{\rm ela} = +\infty, \quad \lim_{\lambda_i\to 0} \varepsilon^{\rm ela} = +\infty. \tag{4}$$

If the system is, in addition, incompressible, then an infinite amount of stretching or compression automatically has, as a consequence, an infinite compression/stretching into at least one other direction.

For the discussion of the derivatives of $\varepsilon^{\rm ela}$ with respect to λ_i it is useful to introduce three abbreviations ($i = 1,2,3$)

$$e_i \equiv \left.\frac{\partial \varepsilon^{\rm ela}}{\partial \lambda_i}\right|_{\lambda_j,\lambda_k=\text{const.}} \equiv \left.\frac{\partial \varepsilon}{\partial \lambda_i}\right|_{\lambda_j,\lambda_k=\text{const.}} \tag{5}$$

(for $k \neq i \neq j$), which can be viewed as generalized elastic forces. For the undeformed state we consequently have

$$e_i(\lambda_1 = \lambda_2 = \lambda_3 = 1) = 0, \quad i = 1,2,3. \tag{6}$$

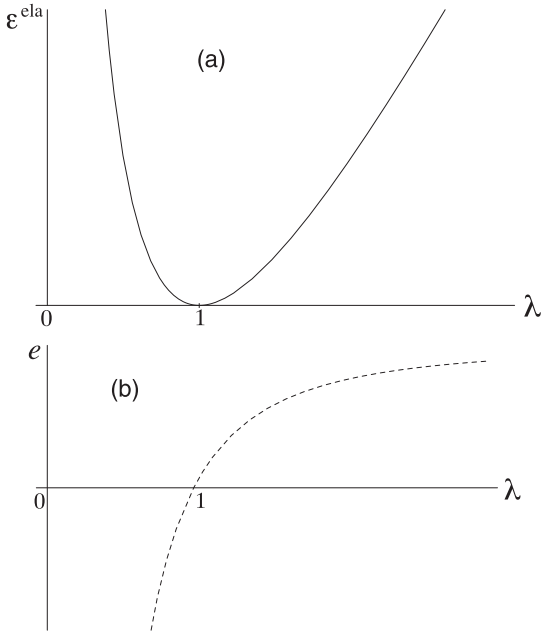

FIG. 1. Schematic behavior of (a) the elastic energy density $\varepsilon^{\rm ela}$ and (b) its first derivative $e = \partial\varepsilon^{\rm ela}/\partial\lambda$ as a function of the one-dimensional stretch ratio λ.

To guarantee that one has a global minimum, the Hessian $H_{ij} = \partial^2\varepsilon^{\rm ela}/(\partial\lambda_i\partial\lambda_j) = \partial e_i/\partial\lambda_j$ at the location $\lambda_1 = \lambda_2 = \lambda_3 = 1$ must be positive definite [15]. The consequences of these properties are sketched for the one-dimensional case in Fig. 1.

A simplification is obtained by the assumption (also used here) that the three functions e_i depend only on the associated stretch ratio, e.g., e_1 is only a function of λ_1. This is equivalent to the assumption that the energy has no coupling terms between the different λ_i's. Based on the symmetry requirements already discussed, the three functions $e_i(\lambda_i)$ with $i = 1,2,3$ are converted into each other when the indices are interchanged. The e_i values have the properties that they have a 0 at $\lambda_i = 1$ and a positive slope at this point [compare also Fig. 1(b)]. If the system is, in addition, thermodynamically stable for arbitrary deformations [15], then H_{ij} is positive at every point, or phrased differently, the e_i's are monotonically growing functions of λ_i. Taken together this implies, for the $e_i(\lambda_i)$,

$$\begin{aligned} e_i &< 0 \quad \text{for} \quad 0 < \lambda_i < 1, \\ e_i &= 0 \quad \text{for} \quad \lambda_i = 1, \\ e_i &> 0 \quad \text{for} \quad \lambda_i > 1. \end{aligned} \tag{7}$$

A decisive advantage gained by the introduction of the e_i becomes obvious when the elastic part of the stress tensor, $\sigma_{ij}^{\rm ela}$ [1], is inspected:

$$\sigma_{ij}^{\rm ela} = U_{ik}\psi_{kj} + U_{jk}\psi_{ik} - \psi_{ij}. \tag{8}$$

The influence of the energy is expressed by the elastic stresses $\psi_{ij} = \partial\varepsilon/\partial U_{ij}$, meaning by six initially unknown functions of U_{ij}. Due to the introduction of the e_i's we can reduce this number to three, making the structure of the stress tensor

clearer. Using the chain rule we can express the ψ_{ij} by the e_i:

$$\psi_{ij} = e_k \frac{\partial \lambda_k}{\partial U_{ij}}. \tag{9}$$

The stretch coefficients are related to the eigenvalues U_i of the strain tensor by [12] $\lambda_i = 1/\sqrt{1-2U_i}$. Since we need, for our further discussion, the explicit dependence of the λ_i on U_{ij}, we consider shear and elongational flows separately, for simplicity. The eigenvalues U_i for a shear flow are given by the equations

$$U_1 = \tfrac{1}{2}(U_{xx} + U_{yy} - U), \tag{10}$$

$$U_2 = \tfrac{1}{2}(U_{xx} + U_{yy} + U), \tag{11}$$

with the abbreviation U,

$$U \equiv \sqrt{(U_{xx} - U_{yy})^2 + 4U_{xy}U_{yx}} \tag{12}$$

[compare [1] for further details]. From Eq. (9) we then find, for the nonvanishing components of ψ_{ij},

$$\psi_{xy} = b\big(-\lambda_1^3 e_1 + \lambda_2^3 e_2\big), \tag{13}$$

$$\psi_{xx} = \tfrac{1}{2}(1-a)\lambda_1^3 e_1 + \tfrac{1}{2}(1+a)\lambda_2^3 e_2, \tag{14}$$

$$\psi_{yy} = \tfrac{1}{2}(1+a)\lambda_1^3 e_1 + \tfrac{1}{2}(1-a)\lambda_2^3 e_2. \tag{15}$$

Since $\lambda_3 = 1$ we have $e_3 = \psi_{zz} = 0$. The abbreviations a and b have been defined via

$$a \equiv \frac{U_{xx} - U_{yy}}{U}, \tag{16}$$

$$b \equiv \frac{U_{xy}}{U}, \tag{17}$$

and we note that these quantities are not independent of each other but satisfy the relation $a^2 + 4b^2 = 1$. Using these relations as well as $\lambda_2 = \lambda_1^{-1}$ for the incompressible case we find from Eq. (8), for the elastic stress tensor,

$$\sigma_{xy}^{\mathrm{ela}} = b\big(\lambda_1 e_1 - \lambda_1^{-1} e_2\big), \tag{18}$$

$$\sigma_{xx}^{\mathrm{ela}} = -\tfrac{1}{2}(1-a)\lambda_1 e_1 - \tfrac{1}{2}(1+a)\lambda_1^{-1} e_2, \tag{19}$$

$$\sigma_{yy}^{\mathrm{ela}} = -\tfrac{1}{2}(1+a)\lambda_1 e_1 - \tfrac{1}{2}(1-a)\lambda_1^{-1} e_2. \tag{20}$$

The two normal stress differences $N_1 = \sigma_{xx} - \sigma_{yy}$ and $N_2 = \sigma_{yy} - \sigma_{zz}$ read

$$N_1 = a\big(\lambda_1 e_1 - \lambda_1^{-1} e_2\big), \tag{21}$$

$$N_2 = -\tfrac{1}{2}(1+a)\lambda_1 e_1 - \tfrac{1}{2}(1-a)\lambda_1^{-1} e_2. \tag{22}$$

Based on the structures derived so far, one can draw several conclusions about the general properties of the stress. For example, from Eqs. (18) and (21) we obtain the interesting relation

$$\frac{\sigma_{xx}^{\mathrm{ela}} - \sigma_{yy}^{\mathrm{ela}}}{\sigma_{xy}^{\mathrm{ela}}} = \frac{U_{xx} - U_{yy}}{U_{xy}} = \frac{a}{b}. \tag{23}$$

Such a relation is trivial for linear elasticity but holds for general nonlinear systems as well [16]. This relation is particularly interesting, because we can make general statements about the stress tensor without knowing the energy density explicitly. We only need the solutions of the dynamic equations for U_{ij}. Below we make use of this possibility.

Based on the properties of the e_i we can obtain information about the sign of $\sigma_{xy}^{\mathrm{ela}}$ and N_1. Since U_2 has been defined as the largest eigenvalue, we always have $\lambda_1 < 1$ and $\lambda_1^{-1} > 1$. Together with Eq. (7) it follows immediately that $\lambda_1 e_1 - \lambda_1^{-1} e_2$ is always negative in a deformed system. This inequality is equivalent to the Baker-Ericksen inequality [17,18] for the situation considered here. As a consequence, $\sigma_{xy}^{\mathrm{ela}}$ has the opposite sign of b, and N_1 the opposite sign of a, and we can determine the signs of $\sigma_{xy}^{\mathrm{ela}}$ and N_1 based exclusively on the structure of the strain tensor. For example, for a stationary shear flow a is positive, thus, the first normal stress difference must always be negative. On the contrary, $\sigma_{xy}^{\mathrm{ela}}$ changes sign with the shear direction, e.g., for positive shear rates the elastic shear stress is negative, while for negative shear rates the elastic shear stress is positive. For the second normal stress difference such a discussion of the sign is not possible, since the two contributions have different signs and therefore the sign of the whole expression can be positive or negative.

For elongational flow the result is much simpler, since the strain tensor is diagonal. In the notation of (I) [1] we have, for ψ_{ij},

$$\psi_{xx} = \psi_{yy} = \lambda_1^3 e_1, \tag{24}$$

$$\psi_{zz} = \lambda_1^{-3} e_2, \tag{25}$$

and all off-diagonal elements vanish. The experimentally relevant normal stress difference takes the simple form

$$\sigma_{zz}^{\mathrm{ela}} - \sigma_{xx}^{\mathrm{ela}} = \lambda_1 e_1 - \lambda_1^{-1} e_2. \tag{26}$$

Combining Eq. (26) with Eq. (7) we conclude that in a uniaxial elongational flow the normal stress difference is always negative, while it is always positive for a biaxial elongational flow.

III. CONSTRUCTION OF AN ENERGY DENSITY APPLICABLE TO LARGE DEFORMATIONS

Before beginning with the construction of a generalized elastic energy density valid for large deformations, we recall the expansion used for small deformations in the companion paper [1]:

$$\varepsilon^{\mathrm{rf}}(s,\rho,U_{ij}) = \bar{\varepsilon}(s,\rho) + \tfrac{1}{2}K_1 \mathrm{Tr}(\mathbf{U}^2) + \tfrac{1}{3}K_2 \mathrm{Tr}(\mathbf{U}^3) + \tfrac{1}{4}K_3 \mathrm{Tr}(\mathbf{U}^4). \tag{27}$$

This expression reads explicitly

$$\varepsilon_{\mathrm{ent}}^{\mathrm{ela}} = \tfrac{1}{2}K_1\big(U_1^2 + U_2^2 + U_3^2\big) + \tfrac{1}{3}K_2\big(U_1^3 + U_2^3 + U_3^3\big) + \tfrac{1}{4}K_3\big(U_1^4 + U_2^4 + U_3^4\big). \tag{28}$$

Following the Cayley-Hamilton theorem, Eq. (27) can be recast in a different form using the three invariants of the symmetric three-dimensional tensor U_{ij} (compare, for example, Refs. [19] and [20]). We note that this leaves the number of independent coefficients unchanged in the compressible case.

If we want to apply this energy density to strongly deformed systems, we encounter two major problems:

1. The region of validity of this expansion is rather limited. As we have seen, for the elastic parameters we have $K_2 \approx 4.5K_1$ and $K_3 \approx 15K_1$, which means that the expansion coefficients in Eq. (28) increase by a factor of about 2.5 to 3 at every order.

2. The behavior for large deformations is not given correctly by Eq. (28). If the system is, for example, infinitely stretched along the first principal axis, then the expansion coefficient λ_1 diverges and the energy density should diverge. However, the associated eigenvalue U_1 goes to 1/2 and $\varepsilon_{\text{ent}}^{\text{ela}}$ stays finite.

Our approach is now, starting with Eq. (28), to find a generalization which is as simple as possible, removes the difficulties described, and satisfies the thermodynamic properties listed in Sec. II. Furthermore, the expansion of the new energy up to fourth order in the eigenvalues U_i should coincide with Eq. (28).

One possibility for finding an elastic energy for polymeric fluids comes from the field of rubber elasticity [12–14]. There are numerous empirical expressions of the elastic energy of an isotropic soft solid as a function of the expansion coefficients λ_1, λ_2, and λ_3, starting with the work of Rivlin [21]. While it is not mandatory that the same elastic energy applies for polymeric fluids and solids; on the other hand, this is an ansatz which has a lot of appeal.

A very simple expression goes back to Mooney [22] and reads

$$\varepsilon_{\text{M}}^{\text{ela}} = \tilde{C}_1\big(\lambda_1^2+\lambda_2^2+\lambda_3^2-3\big) + \tilde{C}_2\big(\lambda_1^{-2}+\lambda_2^{-2}+\lambda_3^{-2}-3\big). \tag{29}$$

One sees immediately that this expression gives the behavior for large deformations qualitatively correctly. Since the energy density has only two elastic parameters, while our expansion $\varepsilon_{\text{ent}}^{\text{ela}}$ has three, we have to verify, first, whether an expansion of $\varepsilon_{\text{M}}^{\text{ela}}$ reduces to $\varepsilon_{\text{ent}}^{\text{ela}}$ so that all requirements for K_1, K_2, and K_3 can be satisfied. To check this we expand Eq. (29) into U_1, U_2, and U_3 up to fourth order and compare the result with Eq. (28). In doing this we must take into account that Mooney's energy assumes incompressibility [22]. We therefore express U_3 with the incompressibility conditions $(1-2U_1)(1-2U_2)(1-2U_3)=1$ in terms of U_1 and U_2 and insert the result into $\varepsilon_{\text{ent}}^{\text{ela}}$. Equation (28) then takes the form

$$\begin{aligned}\varepsilon_{\text{ent}}^{\text{ela}} \approx\ & K_1\big(U_1^2+U_2^2+U_1U_2\big) + 2K_1\big(U_1^3+U_2^3\big)\\ &+\big(4K_1-K_2\big)\big(U_1^2U_2+U_1U_2^2\big)\\ &+\big(6K_1-2K_2+\tfrac{1}{2}K_3\big)\big(U_1^4+U_2^4\big)\\ &+(12K_1-6K_2+K_3)\big(U_1^3U_2+U_1U_2^3\big)\\ &+\big(14K_1-8K_2+\tfrac{3}{2}K_3\big)U_1^2U_2^2.\end{aligned} \tag{30}$$

Comparing this expression with the corresponding result of the expansion of Eq. (29), we can express the two parameters $\tilde{C}_1$ and $\tilde{C}_2$ with K_1 and K_2:

$$\tilde{C}_1 = \tfrac{1}{8}(K_2-2K_1), \tag{31}$$

$$\tilde{C}_2 = \tfrac{1}{8}(4K_1-K_2). \tag{32}$$

In addition, one must require

$$K_3 = 4K_2-4K_1, \tag{33}$$

implying that K_3 can no longer be chosen freely. A comparison with the restrictions found for the values of K_3 in the companion paper (compare Eqs. (30) and (49) in [1]),

$$4K_2-4K_1 < K_3 < 4K_2-2K_1, \tag{34}$$

shows that Eq. (33) coincides with the lower bound of conditions (34). This means that the Mooney energy cannot describe the relaxation behavior of a shear flow in the limit of low shear rates. While $\varepsilon_{\text{M}}^{\text{ela}}$ is therefore not optimum, our consideration shows that our approach is not completely off.

A more severe problem is, however, the fact that the parameter $\tilde{C}_2$ must be negative so that one can satisfy the condition for the occurrence of the Weissenberg effect, $K_2 > 4K_1$. The consequences resulting from this condition become clear using a simple example: if we insert into Eq. (29) the geometry of an elongational flow, that is, $\lambda_1=\lambda_2=\lambda_3^{-1/2}$, then for very small λ_3 the Mooney energy takes the form $\varepsilon_{\text{M}}^{\text{ela}} \approx \tilde{C}_2\lambda_3^{-2}$. Thus the energy becomes negative and tends to $-\infty$ for $\lambda_3 \to 0$, meaning that it behaves unphysically in this regime (cf. also Fig. 3).

Finally, we remark that the Mooney energy has no global minimum in the undistorted state, since one has for all e_i $(\lambda_i = 1) \neq 0$. This can be traced back to the fact that Eq. (29) only applies to an incompressible system and that therefore the relation $\lambda_1\lambda_2\lambda_3=1$ must be used as an additional constraint to have the global minimum at the correct location. This renders the Mooney expression inappropriate for our purposes.

To address and solve the three problems described we modify the Mooney energy so that the resulting energy is minimal in the undeformed state without the need for an additional constraint. The simplest possibility for realizing this reads

$$\begin{aligned}\varepsilon_{\text{a}}^{\text{ela}} =\ & C_1[(\lambda_1-1)^2+(\lambda_2-1)^2+(\lambda_3-1)^2]\\ &+C_2[(1-\lambda_1^{-1})^2+(1-\lambda_2^{-1})^2+(1-\lambda_3^{-1})^2].\end{aligned} \tag{35}$$

The energy density introduced this way indeed has the desired global minimum as one can see from

$$e_i^{\text{a}} = 2\left(C_1+\frac{C_2}{\lambda_i^3}\right)(\lambda_i-1). \tag{36}$$

From the behavior required for large deformations it follows automatically that

$$C_1 > 0 \quad \text{and} \quad C_2 > 0. \tag{37}$$

In addition, the e_i^{a} are strictly monotonically increasing functions.

The modified Mooney expression also contains only two parameters, which can be expressed by K_1 and K_2 using the same method as before,

$$C_1 = \tfrac{1}{12}(2K_2-3K_1), \tag{38}$$

$$C_2 = \tfrac{1}{12}(9K_1-2K_2), \tag{39}$$

with an additional, but different, condition on K_3:

$$K_3 = 4K_2-\tfrac{7}{2}K_1. \tag{40}$$

In contrast to the previous case, this condition is compatible with interval (34) for K_3. However, because $C_2 > 0$ we obtain

from Eq. (39) the constraint that we can only describe systems for which $K_2 < 4.5K_1$.

We can now express the conditions which we have derived in the companion paper [1] for K_1, K_2, and K_3 in terms of C_1 and C_2. Condition for

(a) shear thinning ($K_3 < 4K_2 - 2K_1$), $C_1 + C_2 > 0$;
(b) the correct sign of Ψ_1 ($K_1 > 0$), $C_1 + C_2 > 0$;
(c) the correct sign of Ψ_2 ($K_2 < 5K_1$), $C_1 + 7C_2 > 0$;
(d) the correct relaxation behavior ($K_3 > 4K_2 - 4K_1$), $C_1 + C_2 > 0$;
(e) the Weissenberg effect ($K_2 > 4K_1$), $C_1 > 5C_2$.

It is remarkable that three of the conditions, which look completely differently for the K_i, are identical in the representation using C_1 and C_2. Since, in addition, C_1 and C_2 are positive, it appears remarkable that all relations except for the condition for the Weissenberg effect are already automatically satisfied.

In concluding this section we investigate how strongly the modified Mooney energy $\varepsilon_{\rm a}^{\rm ela}$ introduced here differs from $\varepsilon_M^{\rm ela}$. To see this we insert the structure of the stretch coefficients for a shear flow ($\lambda_1 = \lambda$, $\lambda_2 = 1/\lambda$, $\lambda_3 = 1$) into both energies:

$$\varepsilon_M^{\rm ela} = (\tilde{C}_1 + \tilde{C}_2)(\lambda^2 + \lambda^{-2} - 2), \tag{41}$$

$$\varepsilon_{\rm a}^{\rm ela} = (C_1 + C_2)[(\lambda - 1)^2 + (1 - \lambda^{-1})^2]. \tag{42}$$

Since $4(\tilde{C}_1 + \tilde{C}_2) = 2(C_1 + C_2) = K_1$, only one elastic constant contributes effectively, and we can plot $\varepsilon_M^{\rm ela}$ and $\varepsilon_{\rm a}^{\rm ela}$ in units of K_1 for the comparison of the energies in Fig. 2. It turns out that both energies differ only quantitatively, and not qualitatively, in the present case. One notes, however, that $\varepsilon_{\rm a}^{\rm ela}$ increases more rapidly.

This situation changes drastically when we compare the energies for a three-dimensional elongational flow ($\lambda_1 = \lambda_2 = \lambda^{-1/2}$, $\lambda_3 = \lambda$):

$$\varepsilon_M^{\rm ela} = \tilde{C}_1(2\lambda^{-1} + \lambda^2 - 3) + \tilde{C}_2(2\lambda + \lambda^{-2} - 3), \tag{43}$$

$$\varepsilon_{\rm a}^{\rm ela} = C_1\left[2\left(\lambda^{-\frac{1}{2}} - 1\right)^2 + (\lambda - 1)^2\right] + C_2\left[2\left(1 - \lambda^{\frac{1}{2}}\right)^2 + (1 - \lambda^{-1})^2\right]. \tag{44}$$

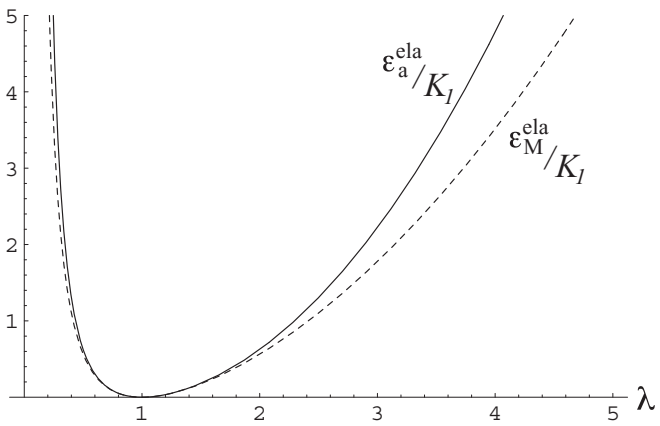

FIG. 2. Energy densities $\varepsilon_M^{\rm ela}$ and $\varepsilon_{\rm a}^{\rm ela}$ in units of K_1 for a planar shear geometry.

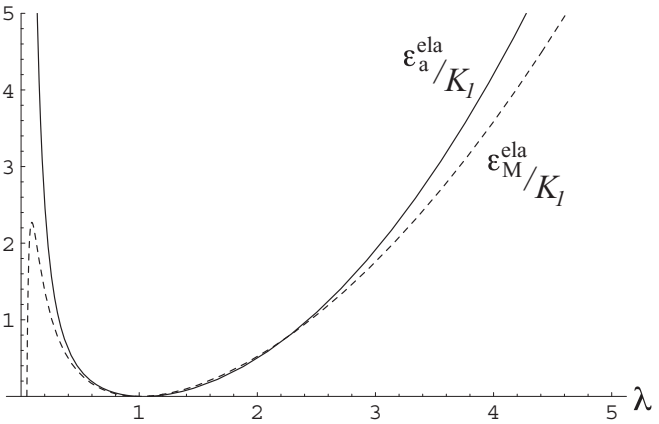

FIG. 3. Energy densities $\varepsilon_M^{\rm ela}$ and $\varepsilon_{\rm a}^{\rm ela}$ in units of K_1 for an elongational geometry. The plot is for $K_2 = 4.2K_1$.

Here we cannot simply represent the energies in terms of K_1. For Fig. 3 we have chosen $K_2 = 4.2K_1$ (this corresponds to $-\Psi_2/\Psi_1 = 0.2$ for low shear rates). For uniaxial elongational flow ($\lambda > 1$) both energies are qualitatively similar; for $\lambda < 1$ we see, as expected, that the Mooney energy goes through a maximum; and for $\lambda \to 0$ it tends to $-\infty$. In contrast, our modified Mooney energy $\varepsilon_{\rm a}^{\rm ela}$ shows the correct thermodynamic behavior.

IV. SHEAR FLOWS FOR LARGE STRAINS

We now have the possibility—using the energy derived in the preceding section—to reach the domain of high shear rates $\dot{\gamma}(t) = \nabla_y v_x(y,t)$ for planar shear flow. This means we can go beyond the limit $|\xi| \ll 1$ for the dimensionless shear rate $\xi \equiv \tau\dot{\gamma}$ [with τ the relaxation time of Eq. (1)], which we had to impose in the companion paper [1]. We discuss stationary and relaxing shear flow as well as the onset behavior with the newly determined stress tensor; the strain tensor is the same as in part (I).

Before we discuss the examples, we use the generalized elastic forces e_i defined in Eq. (5) and the relations (18), (21), and (22) introduced and evaluated in the preceding section to obtain general expressions for $\sigma_{xy}^{\rm ela}$, N_1, and N_2. We make use of the fact that for planar shear flow $\lambda_3 = 1$ and $\lambda_1\lambda_2 = 1$. Using the modified energy $\varepsilon_{\rm a}^{\rm ela}$ we have

$$\sigma_{xy}^{\rm ela} = 2(C_1 + C_2)b(\lambda_1 - \lambda_2)(\lambda_1 + \lambda_2 - 1)\,, \tag{45}$$

$$N_1 = 2(C_1 + C_2)a(\lambda_1 - \lambda_2)(\lambda_1 + \lambda_2 - 1)\,, \tag{46}$$

$$N_2 = -(C_1 - C_2)\left[\left(\lambda_1^2 - \lambda_1\right) + \left(\lambda_2^2 - \lambda_2\right)\right] - (C_1 + C_2)a\left[\left(\lambda_1^2 - \lambda_1\right) - \left(\lambda_2^2 - \lambda_2\right)\right], \tag{47}$$

where the normalized strain components a and b are defined in Eqs. (16) and (17). This result has a remarkable feature: The elastic shear stress and the first normal stress difference depend effectively only on one elastic constant, namely, $C_1 + C_2 = (1/2)K_1$.

With these preparations we are now ready to discuss the three examples separately. For the plots in this section we use $K_2 = 4.4K_1$. This relation also implies that the ratio $-\Psi_2/\Psi_1$

has, for vanishing shear rate, the value 0.15, $K_3 = 14.1K_1$, and $29\,C_2 = C_1$. For the plots it is useful to express the parameters in K_1, namely, $C_1 = (29/60)K_1$ and $C_2 = (1/60)K_1$.

A. Stationary shear flow

The strain field of a stationary shear flow follows from Eq. (1) and has been calculated in part (I) [1]:

$$\lambda_1 = \sqrt{\sqrt{1+\xi^2} - |\xi|}, \tag{48}$$

$$\lambda_2 = \sqrt{\sqrt{1+\xi^2} + |\xi|}, \tag{49}$$

$$a = \frac{|\xi|}{\sqrt{1+\xi^2}}, \tag{50}$$

$$b = \frac{\mathrm{sign}(\xi)}{2\sqrt{1+\xi^2}}. \tag{51}$$

We start our discussion with the shear viscosity $\eta = -\sigma_{xy}/\dot{\gamma}$, where $\sigma_{xy} = \sigma_{xy}^{\mathrm{ela}} - \eta_\infty\dot{\gamma}$. A straightforward calculation gives the expression

$$\eta = \eta_\infty + \frac{(C_1+C_2)\tau}{\xi\sqrt{1+\xi^2}}(2\xi - R_+ + R_-), \tag{52}$$

with $R_\pm = (\sqrt{1+\xi^2} \pm \xi)^{1/2}$ and where the first part is the Newtonian viscosity η_∞ and the second part comes from Eq. (45).

The behavior of η as a function of the shear rate is shown in Fig. 4. Since the viscosity depends effectively on only one elastic constant, the curve obtained is universal and possesses two basic features: It is monotonically decreasing and thus shows the typical shear thinning behavior [2], and for large values of ξ it converges towards the constant η_∞. Experimentally it is well established [2] that the shear viscosity can decrease by several orders of magnitude. From Eq. (52) we see that $\eta \to \eta_\infty$ for $\xi \to \infty$; it can decrease by orders of magnitude for $\eta_\infty \ll K_1\tau$.

For comparison we have plotted as a dashed line the result of the expansion for low shear rates obtained in part (I) [1],

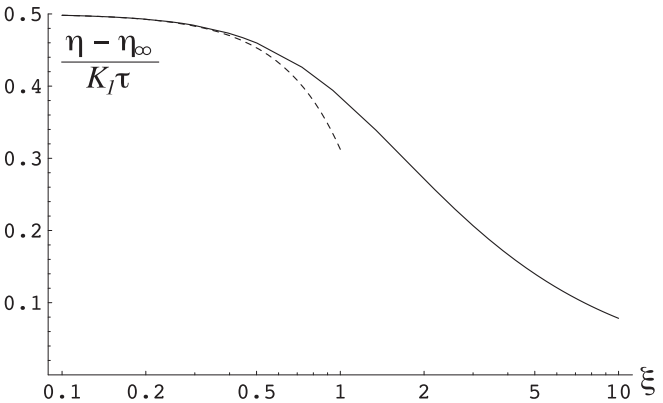

FIG. 4. The shear viscosity η in units of $K_1\tau$ as a function of the dimensionless shear rate ξ. The dashed curve represents the solution of the expansion up to second order in ξ part (I) [1].

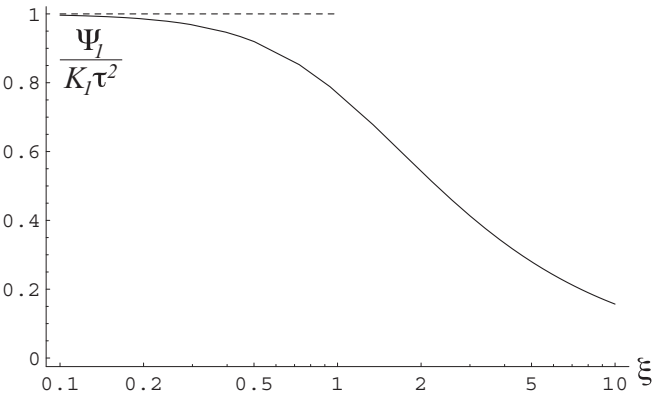

FIG. 5. The first normal stress coefficient Ψ_1 in units of $K_1\tau^2$ as a function of the dimensionless shear rate ξ. The dashed horizontal line represents the result in part (I) [1].

using $K_3 = 4K_2 - (7/2)K_1$,

$$\eta = \eta_\infty + \tfrac{1}{2}K_1\tau\left(1 - \tfrac{3}{8}\xi^2\right) + \mathcal{O}(\xi^4), \tag{53}$$

which again depends only on K_1, so that Fig. 4 is applicable for arbitrary values of K_2 in the admissible range. The first normal stress difference $\Psi_1 = -N_1/\dot{\gamma}$ assumes a similar shape as η,

$$\Psi_1 = \frac{2(C_1+C_2)\tau^2}{\xi\sqrt{1+\xi^2}}(2\xi - R_+ + R_-), \tag{54}$$

and is a universal function when plotted in units of $K_1\tau^2$ as a function of ξ (Fig. 5). Similarly, as the viscosity, Ψ_1 is also a monotonically decreasing function of the shear rate. In contrast to the viscosity, however, the normal stress coefficient goes to 0 for $\xi \to \infty$, and not to a finite value. This behavior is in accord with available experimental data [2]. The result obtained by the energy expansion in part (I) [1] is plotted as the dashed horizontal line. It is a constant, since one would have to expand the energy density to fifth order to get a ξ dependence.

The similarity of the ξ dependence of $\eta - \eta_\infty$ and Ψ_1 is neither accidental nor a result of the special form of our energy, but is universal. Using the energy-independent relation, Eq. (23), for shear flows, we immediately get, with Eqs. (50) and (51),

$$\frac{N_1}{\sigma_{xy} + \frac{\eta_\infty}{\tau}\xi} = 2\xi. \tag{55}$$

For low shear rates $N_1 = 2\xi\sigma_{xy}$ and the material functions η and Ψ_1 differ only by the constant factor 2τ. With increasing shear rate, the η_∞ contribution becomes more and more important (due to shear thinning) so that η and Ψ_1 differ not by just a constant, a feature that is also observed experimentally [2]. For the ratio N_1/σ_{xy} this means that with increasing shear rate it first grows linearly and then flattens out gradually [2].

B. Relaxing shear flow

The relaxation behavior of the strain for low shear rates has been discussed in part (I) [1]. Assuming a constant shear flow $\dot{\gamma}_0$ that is instantaneously switched off at time $t = 0$ the strain

field for time $t > 0$ is found from Eq. (1) and takes the form

$$\lambda_1 = \sqrt{\sqrt{1+\xi_0^2\, e^{-2d}} - |\xi_0\, e^{-d}|}, \tag{56}$$

$$\lambda_2 = \sqrt{\sqrt{1+\xi_0^2\, e^{-2d}} + |\xi_0\, e^{-d}|}, \tag{57}$$

$$a = \frac{|\xi_0|}{\sqrt{1+\xi_0^2}}, \tag{58}$$

$$b = \frac{\mathrm{sign}(\xi_0)}{2\sqrt{1+\xi_0^2}}, \tag{59}$$

where $\xi_0 \equiv \dot\gamma_0\tau$ is the dimensionless shear rate and $d \equiv t/\tau$ is the dimensionless time.

The material function (for $t > 0$) $\eta^- = -\sigma_{xy}/\dot\gamma_0$ is now time dependent and has the same structure as $\eta - \eta_\infty$ in the stationary case,

$$\eta^- = \frac{(C_1+C_2)\tau}{\xi_0\sqrt{1+\xi_0^2}}\left(2\xi_0 e^{-d} - S_+ + S_-\right), \tag{60}$$

with $S_\pm = (\sqrt{1+\xi_0^2 e^{-2d}} \pm \xi_0 e^{-d})^{1/2}$ and can be plotted equally well universally (Fig. 6).

We are interested in the question how the relaxation behavior of η^- is influenced by higher values of $|\xi_0|$. In our discussion for the case of small shear rates in part (I) [1] we have seen that the property that η^- relaxes more rapidly for larger values of $|\xi_0|$ is captured well by our model. The relaxation behavior of η^- relative to the initial value $\eta^-(\xi_0,0) = \eta(\xi_0) - \eta_\infty$ for several shear rates is plotted in Fig. 6. All curves are relaxing monotonically to 0.

It turns out that for $|\xi_0| \gg 1$ we have

$$\frac{\eta^-}{\eta - \eta_\infty} \approx e^{-d}. \tag{61}$$

Thus the behavior of the curve is almost independent of shear rate in the limit of high initial shear rates, while the experiments show a stronger dependence [23]. It emerges that a modified equation for U_{ij} will be necessary to account for this observation.

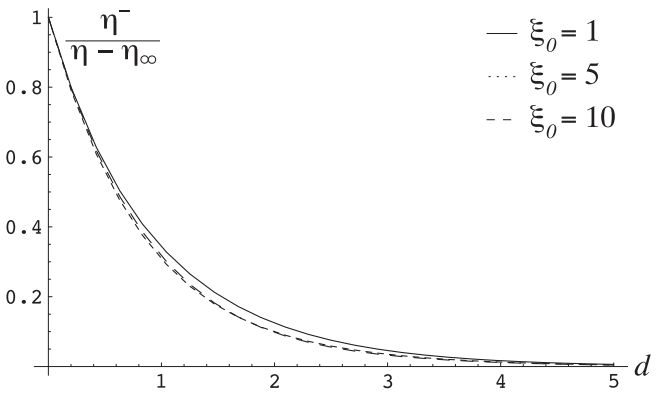

FIG. 6. The material function η^- relative to its stationary value $\eta - \eta_\infty$ as a function of the dimensionless time d for various shear rates.

C. The onset of shear flow

We assume no flow for $t < 0$ and an instantaneously switched-on constant shear flow $\dot\gamma_0$ for $t > 0$. In part (I) it is shown that in this case the set of equations that determines the strain components or the stretch ratios (as functions of $\dot\gamma_0$) is nonlinear and no analytic result can be given [1]. For low shear rates $\xi_0 = \dot\gamma_0$ an expansion in powers of ξ_0 has been used, but here we are interested in the case of large ξ_0 and only a numerical solution is possible. The results for $\xi_0 = 1$ and $\xi_0 = 10$ are shown in Fig. 7, where the stretch ratios λ_1 and λ_2 are given as functions of time.

In the case of low shear rates both quantities are monotonous functions of d (compare the corresponding figures in part (I) [1]). Here, however they show a pronounced overshoot behavior; i.e., they go through one or more minima or maxima before they converge towards their stationary values. This effect is more significant for higher ξ_0.

A similar behavior is found for the material functions $\eta^+ = -\sigma_{xy}/\dot\gamma_0$ and $\Psi_1^+ = -(\sigma_{xx} - \sigma_{yy})/\dot\gamma_0^2$, both experimentally [24,25] and in our description using Eqs. (45) and (46). They are evaluated again numerically and shown in dimensionless form in Figs. 8 and 9.

In particular, the height of the maxima grows with the shear rate (note the different vertical scales) and shifts to shorter values of time. From the measured curves presented in Ref. [2] one sees that for a fixed value of ξ_0 the overshoot of Ψ_1^+/Ψ_1 is higher than that of η^+/η, while in our plots η^+/η has the more pronounced maximum. Therefore we cannot make a quantitative comparison as already expected.

The temporal behavior of the material function $\Psi_2^+ = -(\sigma_{yy} - \sigma_{zz})/\dot\gamma_0^2$ for $\xi_0 = 1$ and $\xi_0 = 10$ is plotted in Fig. 10. As already shown for low shear rates in part (I), Ψ_2^+/Ψ_2 is negative for small times, which means that Ψ_2^+ is positive [1]. With increasing time Ψ_2^+/Ψ_2 changes its sign and converges after an overshoot towards its stationary value. We note that the negative range of Ψ_2^+/Ψ_2 becomes smaller for a higher shear rate. For the overshoot we find the same behavior as before for η^+ and Ψ_1^+: for growing shear rate the overshoot becomes more pronounced and moves to shorter times. Clearly, this can be traced back to the behavior of the strains.

V. ELONGATIONAL FLOW FOR LARGE DEFORMATIONS

Similarly to shear flow we can also generalize our discussions in part (I) for elongational flows using the generalized energy density [1]. We consider a three-dimensional rotational invariant elongational flow of the form $v_x = -\frac{1}{2}\dot\epsilon x$, $v_y = -\frac{1}{2}\dot\epsilon y$, and $v_z = \dot\epsilon z$. For positive $\dot\epsilon$ this describes a uniaxial elongation along the z axis, while for negative ones it is a biaxial elongation in the x-y plane. As known from part (I), in elongational flows the normal stress difference $\sigma_{zz} - \sigma_{xx}$ is the important measurable quantity [1]. From Eq. (26) and the expression for e_i from Eq. (36) we find for the elastic part

$$\sigma_{zz}^{\mathrm{ela}} - \sigma_{xx}^{\mathrm{ela}} = 2C_1[\lambda_1(\lambda_1-1) - \lambda_2(\lambda_2-1)] + 2C_2\left(\frac{\lambda_1-1}{\lambda_1^2} - \frac{\lambda_2-1}{\lambda_2^2}\right). \tag{62}$$

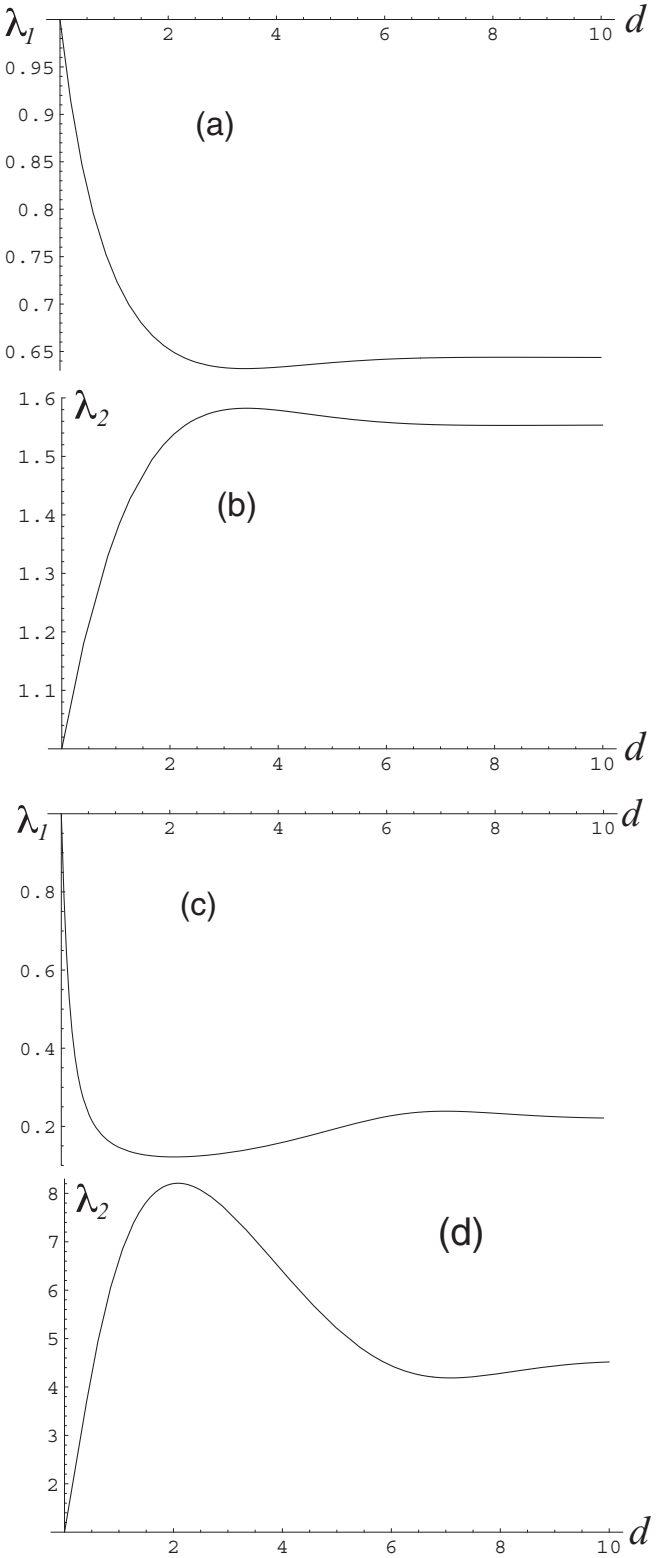

FIG. 7. The stretch ratios λ_1 and λ_2 as a function of the dimensionless time d for (a, b) $\xi_0 = 1$ and (c, d) $\xi_0 = 10$.

For the following plots we use the same numbers for C_1 and C_2 as in the section on shear flows, $C_1 = (29/60)K_1$ and $C_2 = (1/60)K_1$.

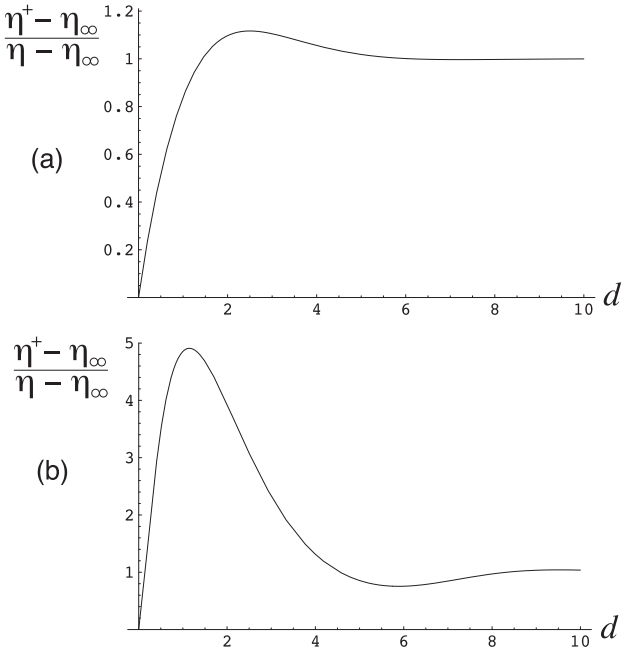

FIG. 8. The material function η^+ relative to the stationary value η as a function of the dimensionless time d for (a) $\xi_0 = 1$ and (b) $\xi_0 = 10$, where $K_2 = 4.4K_1$.

A. Stationary elongational flow

The stretch ratios λ_1 and λ_2 for general $\dot{\epsilon}$ have been found in part (I) [1]:

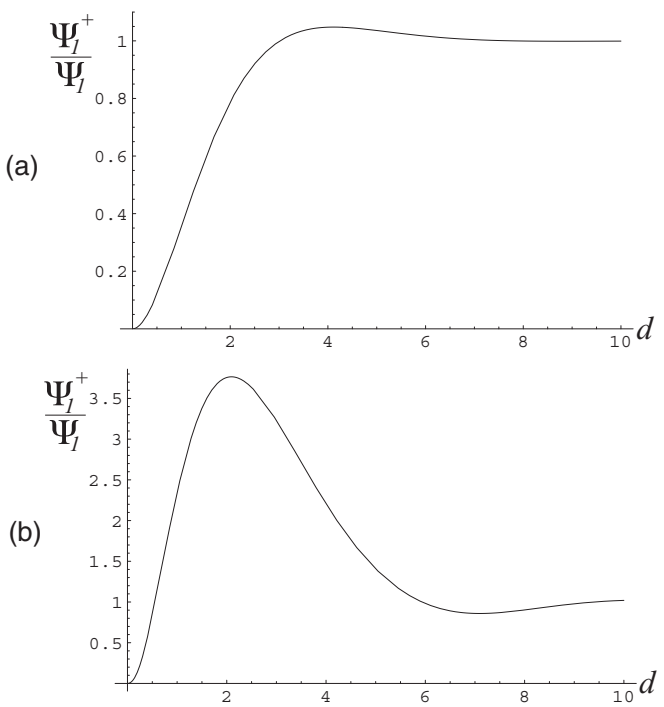

FIG. 9. The material function Ψ_1^+ relative to its stationary value Ψ_1 as a function of the dimensionless time d for (a) $\xi_0 = 1$ and (b) $\xi_0 = 10$, where $K_2 = 4.4K_1$.

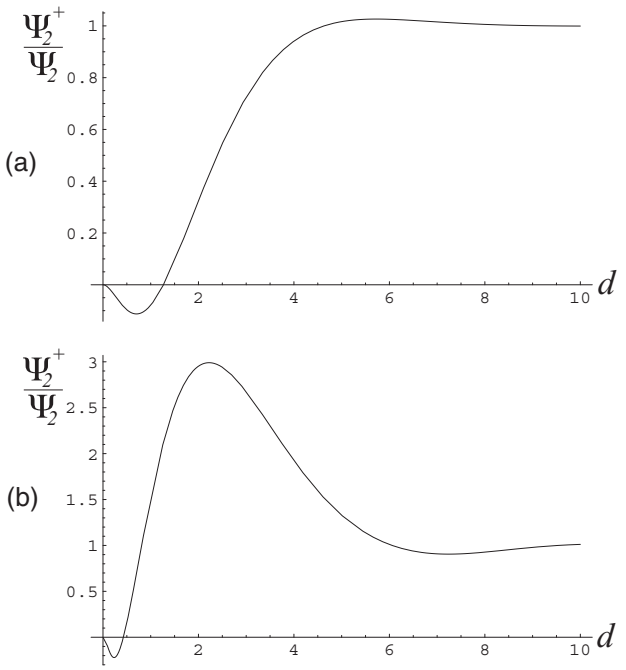

FIG. 10. The material function Ψ_2^+ relative to its stationary value Ψ_2 as a function of the dimensionless time d for (a) $\xi_0 = 1$ and (b) $\xi_0 = 10$, where $K_2 = 4.4K_1$.

$$\lambda_1 = \left(\frac{1-\zeta}{1+2\zeta}\right)^{1/6}, \tag{63}$$

$$\lambda_2 = \left(\frac{1+2\zeta}{1-\zeta}\right)^{1/3}. \tag{64}$$

For a stationary solution to exist, the dimensionless elongation rate $\zeta \equiv \dot{\epsilon}\,\tau$ can only assume values in the interval

$$-\tfrac{1}{2} < \zeta < 1. \tag{65}$$

The Trouton viscosity $\bar{\eta} = -(\sigma_{zz} - \sigma_{xx})/\dot{\varepsilon} = 3\eta_\infty - (\sigma_{zz}^{\rm ela} - \sigma_{xx}^{\rm ela})/\dot{\varepsilon}$ can be calculated from Eq. (62). Since the analytical result is a cumbersome expression, we plot the numerical solution in Fig. 11 as a function of ζ. For comparison, we show the parabola, which resulted from the energy expansion in part (I) [1].

The Trouton viscosity diverges near the boundaries of the existence range for stationary elongation flow rates—in contrast to the results obtained from the energy expansion in part (I) [1]. For a uniaxial elongation flow such a rapid increase is not observed experimentally; the curves end rather abruptly instead [2,14]. For biaxial elongational flows, however, one indeed observes a very strong increase in the viscosity beyond the minimum [26]. For the location of the increase the prediction of various constitutive models is also a dimensionless elongation rate of 1/2 [26,27]. Therefore our model fits well into the existing picture.

B. Onset of elongational flow

A high elongation rate means, in particular, that $\dot{\varepsilon}$ is outside the range, Eq. (65), for which a spatially homogeneous stationary solution for the strain exists. Dealing with the onset of an elongational flow, $\dot{\varepsilon} = 0$ for $t < 0$ and $\dot{\varepsilon} = \dot{\varepsilon}_0$ for $t > 0$, we focus on the different behavior for elongation rates inside and outside of this range.

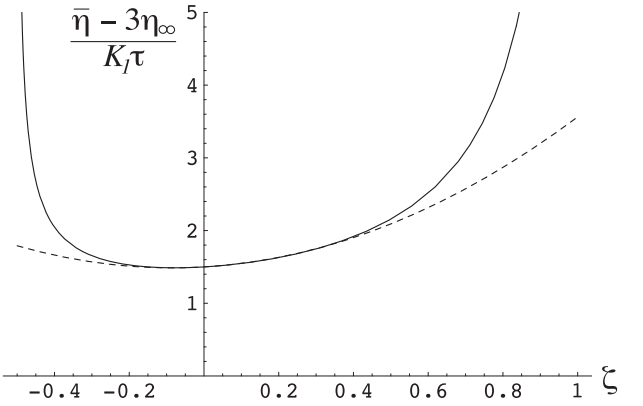

FIG. 11. The Trouton viscosity $\bar{\eta}$ is plotted in units of $K_1\tau$ as a function of the dimensionless elongation rate ζ. The dashed line represents the solution of the energy expansion from part (I) [1]. For both curves we have used $K_2 = 4.4K_1$.

Similarly to the onset of shear flow, there is no analytic solution for the onset of elongational flow. Nevertheless, one can reach some general conclusions using numerical solutions. For the onset of uniaxial elongational flow in the regime where stationary flow exists, i.e., for $0 < \zeta_0 < 1$, the stretch coefficients λ_1 and λ_2 show no overshoot and approach monotonically an asymptotic value [cf. Fig. 12(a)]. A similar behavior was found for the small-ζ_0 expansion in part (I) [1].

For the range $\zeta_0 > 1$ the behavior of λ_1 and λ_2 changes qualitatively. There is no longer a stationary state for finite deformations. λ_1 approaches 0 for $d \to \infty$ and λ_2 tends to $+\infty$ with increasing time d. We see in Fig. 12(b) that λ_1 and λ_2 are monotonic functions of time. We also note that for higher elongation rates they decrease and increase more rapidly, respectively.

For biaxial elongation flow (negative ζ_0) $\lambda_1 > \lambda_2$, but for $d \to \infty$ both converge towards a limiting value if $\zeta_0 > -0.5$. This temporal behavior of λ_1 and λ_2 is plotted in Fig. 13(a). We note that λ_1 and λ_2 are monotonous functions of time: there is no overshoot for a biaxial flow either.

For $\zeta_0 < -0.5$, for which no stationary solution exists, we find that the stretch ratio λ_1 diverges while λ_2 tends to 0 for $d \to \infty$. This behavior is shown in Fig. 13(b). Similarly to a uniaxial extensional flow the stretch ratios grow or decrease more rapidly with time when the magnitude of ζ_0 is larger.

After evaluating the stretch ratios λ_1 and λ_2 we can now determine the time-dependent elongational viscosity $\bar{\eta}^+(\zeta_0, d) = -(\sigma_{zz} - \sigma_{xx})/\dot{\varepsilon}_0$. Both the uniaxial and the biaxial elongation flow [Figs. 14(a) and 14(b), respectively] show two distinct regimes, depending on whether or not stationary elongational flow exists. In the latter region the Trouton viscosity grows monotonically and converges to its value for a stationary elongational flow.

In the former region, the elongational viscosity diverges for $d \to \infty$. In Fig. 14 this divergence appears as an abrupt increase in $\bar{\eta}^+$, which is shifted to shorter times for higher

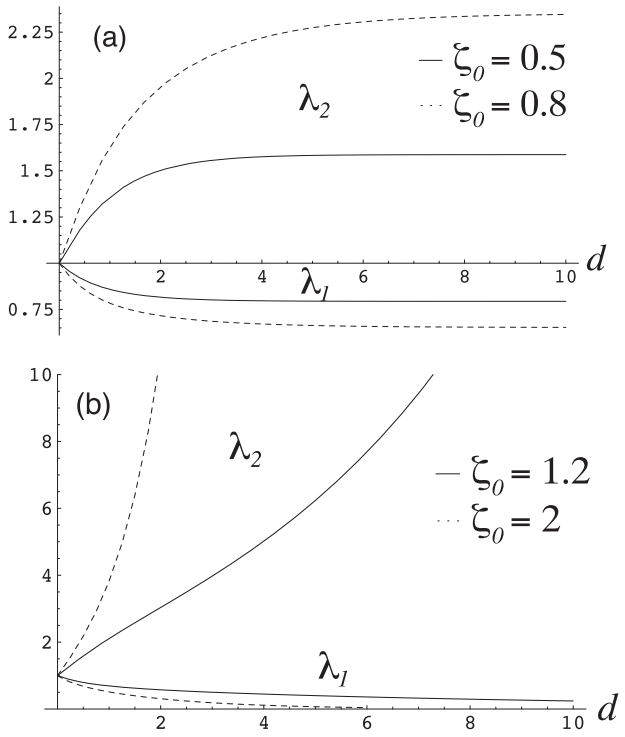

FIG. 12. Behavior of the stretch coefficients λ_1 and λ_2 for a uniaxial elongational flow as a function of the dimensionless time, d, for different ζ_0's. (a) Values of ζ_0 for which a stationary state exists ($0 < \zeta_0 < 1$). (b) Values of ζ_0 for which no stationary state exists ($\zeta_0 > 1$).

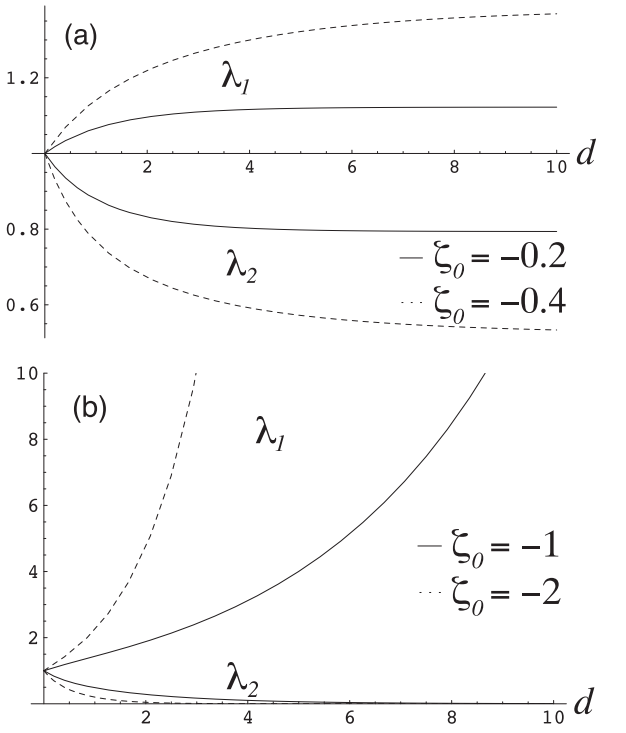

FIG. 13. Behavior of the stretch ratios λ_1 and λ_2 for a biaxial elongational flow as a function of the dimensionless time d for various values of ζ_0. (a) Values of ζ_0 for which a stationary state exists ($-1/2 < \zeta_0 < 0$). (b) Values of ζ_0 for which there is no stationary state ($\zeta_0 < -1/2$).

elongation rates $\dot{\varepsilon}_0$. This effect is known as "strain hardening" [2] and is qualitatively well accounted for in our model.

From experiments one finds, for the time scale t_c of the abrupt increase,

$$\varepsilon_H = \dot{\varepsilon}_0 t_c = \zeta_0 d_c = \text{const.} \tag{66}$$

ε_H is known as the *Hencky strain* and has different values for different samples [2]. Inspection of Fig. 14 shows that is is difficult within our model to determine d_c precisely, since $\bar{\eta}^+$ grows monotonically and does not break at a specific instant in time. It is clear, however, that relation (66) is roughly satisfied, since d_c tends to decrease with increasing ζ_0.

Since we have used a logarithmic time axis in Fig. 14, we see that for short times, that is, for $t \ll \tau$, the behavior of $\bar{\eta}^+(\zeta_0,d)$ is obviously independent of the elongation rate. This property is also known from experimental data [28]. We investigate this feature and expand $\bar{\eta}^+(\zeta_0,d)$ into the dimensionless time d up to second order. For arbitrary values of ζ_0 we find

$$\bar{\eta}^+(\zeta_0,d) = 3\eta_\infty + \tfrac{3}{2}K_1\tau\, d - \tfrac{3}{4}[K_1\tau + (3K_1 - K_2)\tau\zeta_0]d^2. \tag{67}$$

This result is independent of whether one uses the expanded energy density or $\varepsilon_a^{\text{ela}}$. We see that the first-order term depends only on the material parameters, while the dependence on the elongation rate arises only in second order. Therefore the influence of the elongation rate becomes important only for increasing times.

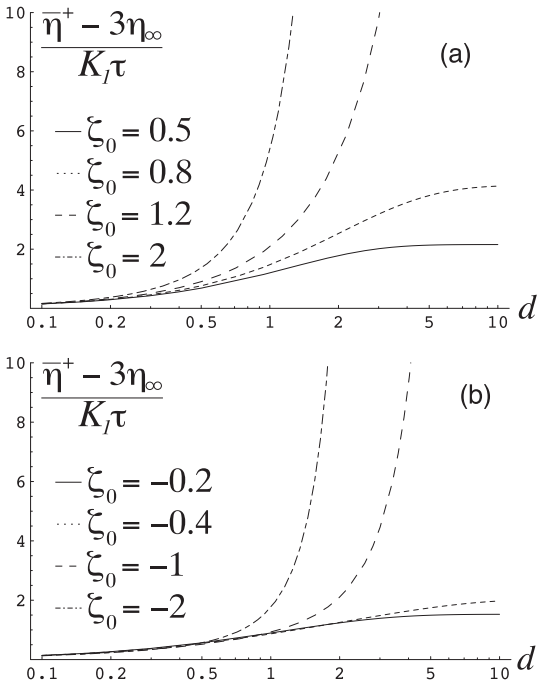

FIG. 14. Onset behavior of the elongational viscosity $\bar{\eta}^+$ as a function of the dimensionless time d for different values of ζ_0 with $K_2 = 4.4K_1$. (a) Uniaxial and (b) biaxial elongational flow.

VI. EMPIRICAL RELATIONS

In rheology, there are a number of empirical relations that connect various material functions of different types of flows. These relations are empirical and typically cannot be derived theoretically. An example, which we have discussed for the linear regime, is the Cox-Merz rule [7]. These relations are frequently used to supplement experimental data with results from experiments, which are easier to perform. In this section we investigate how well our model satisfies some of the best-known relations. The goal is not to explain these empirical relations but, rather, to check our model using a different viewing angle.

A. The Cox-Merz rule

In part (I) we have inspected the Cox-Merz rule [7] for low shear rates [1]. Here we generalize the discussion to higher shear rates. The relation reads

$$\eta(\dot\gamma) = \left|\eta^\star(\tilde\omega = \xi)\right|, \tag{68}$$

with $\tilde\omega = \omega\tau$ the dimensionless frequency of linear oscillatory shear flow. It represents a relation between the shear thinning and the magnitude of the complex viscosity associated with an oscillatory shear flow. In Fig. 15 we compare the solutions for η from Eq. (52) with the expression we obtained in part (I) [1]:

$$|\eta^\star(\tilde\omega = \xi)| = \frac{K_1\tau}{2\sqrt{1+\xi^2}}. \tag{69}$$

We discard the parameter η_∞, since it plays almost no role in the range $\xi \leqslant 10$. As a consequence, the curves for η and $|\eta^\star|$ in Fig. 15 are universal and parameter-free. Both curves show qualitatively the same behavior, however, $|\eta^\star|$ falls off somewhat more rapidly. Given the limited quantitative applicability of the simple expression for the energy density $\varepsilon_a^{\rm ela}$, the result is quite satisfactory.

In Fig. 15 the larger ξ becomes, the more important the influence of the viscosity η_∞. $|\eta^\star|$ then takes the form [compare

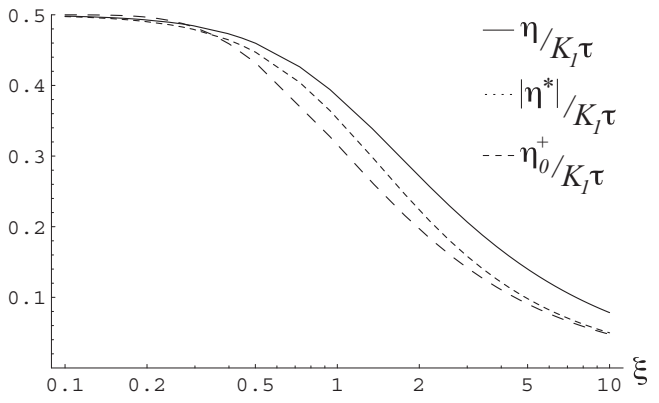

FIG. 15. Comparison of the shear thinning curve $\eta(\xi)$ with $|\eta^\star|$ (Cox-Merz rule) and with η_0^+ (first Gleißle mirror relation) as functions of $\xi = \tilde\omega$. η_∞ has been neglected.

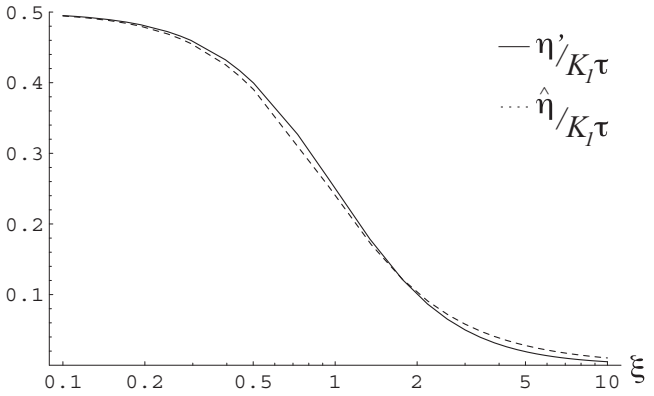

FIG. 16. Comparison of η' and $\hat\eta$ as functions of $\xi = \tilde\omega$.

Eqs. (86) and (87) in part (I)]

$$|\eta^\star| = \sqrt{\eta_\infty^2 + \frac{K_1\tau(K_1\tau + 4\eta_\infty)}{4(1+\tilde\omega^2)}} \tag{70}$$

[1], and we see that this function converges for $\xi = \tilde\omega \to \infty$ to η_∞ as does η. For finite frequencies, however, there is a qualitative difference: for η, η_∞ is simply an additive constant, which has no influence on the shape of the function. This property is independent of the form of the energy and results from $\eta = \eta_\infty - \sigma_{xy}^{\rm ela}/\dot\gamma$ and the fact that η_∞ does not enter $\sigma_{xy}^{\rm ela}$. On the contrary, $|\eta^\star|$ depends on η_∞ in a complex fashion. As a consequence, the viscosity constant influences the shape of $|\eta^\star|$ for higher frequencies. Therefore it is no longer possible to fulfill the Cox-Merz rule exactly, but it is an approximation in this framework.

In the companion paper [1] we have also discussed a variant of the Cox-Merz rule, which connects the linear behavior of an oscillatory flow with the derivative of the shear stress for a stationary flow [7]:

$$\eta'(\omega = \dot\gamma) = -\frac{\partial\sigma_{xy}}{\partial\dot\gamma}(\dot\gamma). \tag{71}$$

The "viscosity" $\hat\eta = -\partial\sigma_{xy}/\partial\dot\gamma$ is easy to calculate from Eq. (53) but leads to a rather lengthy expression, which we do not report explicitly here. The result depends effectively on only one material parameter, $(C_1 + C_2)\tau$. In addition, we note that—in contrast to the usual Cox-Merz rule—the parameter η_∞ is additive for η' as well as for $\hat\eta$ and, therefore, plays no role in the comparison and is discarded in Fig. 16.

We find excellent agreement, even better than for the usual Cox-Merz rule. This result is also in accordance with what we found in the discussion of low shear rates in part (I) [1].

B. Gleißle's mirror relations

In 1980 Gleißle introduced two empirical relations that connect material functions for a stationary shear flow with those for a start-up shear flow [2,8]. They are used to obtain data for $\eta(\dot\gamma)$ and $\Psi_1(\dot\gamma)$ from nonstationary experiments [29]. Especially the first mirror relation was confirmed experimentally quite well [10].

The first relation is a remarkable connection between the shear thinning curve $\eta(\dot\gamma)$ and the limiting curve $\eta_0^+(t)$ for a

start-up shear flow taken at the time given by the reciprocal shear rate [cf. part (I) [1] and Fig. 8]

$$\eta(\dot\gamma) = \eta_0^+(t = 1/\dot\gamma). \tag{72}$$

This relation is also plotted in Fig. 15. The qualitative agreement using our model is equally as good as before for the Cox-Merz rule. We note, however, that η_0^+ falls off somewhat more rapidly. Of special interest is a direct comparison between the curve $|\eta^\star|$ and the curve η_0^+, since both can be calculated from the linear elasticity and, therefore, without using a general expression for the energy density. The clearly visible similarity between the two functions in Fig. 15 is very high and corresponds to experimentally known features [2]. In our model it is not dependent on the choice of parameters but, instead, closely connected to the similarities of the functions $1/\sqrt{1+\xi^2}$ and $1 - e^{-1/\xi}$.

The second mirror relation [8] connects the first normal stress difference for a stationary shear flow Ψ_1,

$$\Psi_1(\dot\gamma) = \Psi_1^+(\dot\gamma_0 = 0, t = k/\dot\gamma), \tag{73}$$

with that of a start-up shear flow for zero shear rate and taken at time $k/\dot\gamma$. In contrast to the first mirror relation, there is a phenomenological dimensionless constant k, which lies experimentally between 2.5 and 3 [2]. There is again good qualitative agreement, but some quantitative differences for $\xi > 1$.

C. The Laun rule

The Laun rule [2,9] provides the empirical possibility of determining the first normal stress difference of a stationary shear flow from the linear data on an oscillatory shear flow,

$$\Psi_1(\dot\gamma) = \frac{2\eta''(\omega)}{\omega}\left[1 + \left(\frac{\eta''(\omega)}{\eta'(\omega)}\right)^2\right]^{0.7}\Bigg|_{\omega=\dot\gamma}. \tag{74}$$

The functions η' and η'' have been calculated in part (I) [1].

If we neglect η_∞, we find, for the right-hand side of Eq. (74),

$$\Psi_1^L(\xi) = \frac{K_1\tau}{(1+\xi^2)^{0.3}}. \tag{75}$$

Figure 17 shows that Ψ_1 of Eq. (54) agrees quite well with the function Ψ_1^L obtained from Laun's rule.

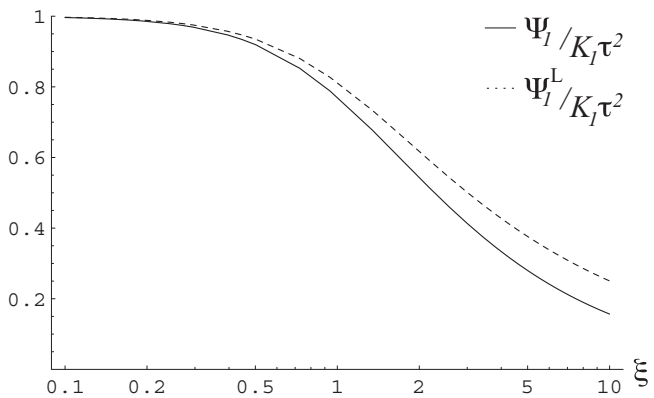

FIG. 17. Comparison of Ψ_1 and Ψ_1^L (Laun's rule) as functions of ξ.

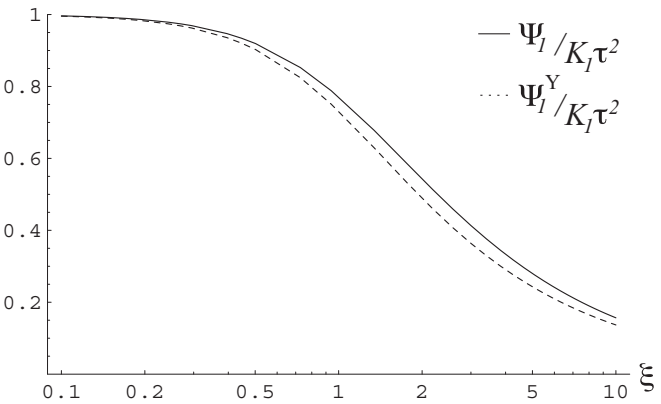

FIG. 18. Comparison of Ψ_1 and Ψ_1^Y (Yamamoto relation) as functions of ξ.

D. The Yamamoto relation

A relation of a somewhat different nature compared to those discussed so far is the Yamamoto relation [10,11]. It connects the viscosity for a relaxing shear flow η^- with the first normal stress difference Ψ_1 for a stationary flow via an integral relation,

$$\Psi_1(\xi) = 2\int_0^\infty \eta^-(\xi, d = T)\mathrm{d}T \equiv \Psi_1^Y(\xi). \tag{76}$$

A comparison of the integral over η^- from Eq. (60) and Ψ_1 from Eq. (54) is shown in Fig. 18. We note that we could not find an analytic solution for Ψ_1^Y.

In this plot the behavior of the curves is again independent of the material properties. The Yamamoto relation is satisfied very well. This is a remarkable result, since we have seen in Sec. IV B that the behavior of $\eta^-(\xi, d)$ is not completely in agreement with experimental results.

VII. CONCLUSIONS AND PERSPECTIVE

In this paper we have applied the systematic model of transient elasticity to the rheology of polymer melts and solutions under large amplitude deformations. Based on a generalized deformation energy applicable for finite strain with only two independent parameters, which reduces to the conventional elastic energy in the limit of small deformations, we have provided qualitative, and frequently even almost-quantitative, agreement with experimental data for many phenomena characteristic of large deformations in polymer rheology. These include viscosity overshoot near the onset of shear flow, the onset of elongational flows in situations for which there is no stationary solution, and shear thinning and normal stress differences for a large range of shear rates. In addition, we find that our model satisfies empirical relations including the Cox-Merz rule, Gleißle's mirror relations, the Laun rule, and the Yamamoto relation, in several cases quantitatively, but always at least qualitatively.

Thus the present work complements nicely the companion paper [1], where the emphasis is on small amplitude deformations. In part (I) we have shown that in the framework of the simplified transient elasticity model valid in the small

strain limit, containing in total five parameters—namely, the relaxation time τ of the transient network, the three elastic constants K_1, K_2, and K_3 associated with the quadratic, cubic, and quartic transient elasticity, and the viscosity parameter η_∞—we could account for many of the experimental observations already occurring for small strains qualitatively and, quite often, even almost quantitatively [1]. These phenomena include, for example, the onset of shear thinning for a stationary shear flow, surface effects including the Weissenberg effect and the surface curvature for the flow down a slightly tilted channel, and predictions about the elongation rate dependence of the Trouton viscosity.

There are several directions in which the results presented could be generalized. One direction is the incorporation of transient orientational elasticity, a concept put forward in [30] that has been compared to classical rheological descriptions in [31]. Another area in which the approach of transient elasticity could turn out to be fruitful is anisotropic composite materials including anisotropic magnetic gels [32,33] as well as liquid crystalline polymers and liquid crystalline elastomers and gels [34–36]. All these systems have a transient network, in many cases in addition to the permanent cross-linking.

ACKNOWLEDGMENTS

H.R.B. and H.P. acknowledge partial support of their work by the Deutsche Forschungsgemeinschaft through SPP 1681 "Feldgesteuerte Partikel-Matrix-Wechselwirkungen: Erzeugung, skalenübergreifende Modellierung und Anwendung magnetischer Hybridmaterialien."

[1] O. Müller, M. Liu, H. Pleiner, and H.R. Brand, Phys. Rev. E **93**, 023113 (2016).
[2] R. B. Bird, R. C. Armstrong, and O. Hassager, *Dynamics of Polymeric Liquids, Vol. 1* (John Wiley, New York, 1987).
[3] K. Weissenberg, Nature **159**, 310 (1947).
[4] D. D. Joseph and R. L. Fosdick, Arch. Rational. Mech. Anal. **49**, 321 (1973).
[5] D. D. Joseph, G. S. Beavers, and R. L. Fosdick, Arch. Rational. Mech. Anal. **49**, 381 (1973).
[6] R. I. Tanner, *Engineering Rheology* (Oxford University Press, New York, 2002).
[7] W. P. Cox and E. H. Merz, J. Polym. Sci. **28**, 619 (1958).
[8] W. Gleißle, in *Rheology, Vol. 2: Fluids*, edited by G. Astarita, G. Marrucci, and L. Nicolais (Plenum Press, New York, 1980), p. S.457ff.
[9] H. M. Laun, J. Rheol. (NY) **30**, 459 (1986).
[10] N. El Kissi, J. M. Piau, P. Attané, and G. Turrel, Rheol. Acta **32**, 293 (1993).
[11] P. Fischer, Dissertation, Universität Essen, 1995.
[12] L. R. Treloar, J. Polym. Sci.: Polym. Symp. **48**, 107 (1974).
[13] A. N. Gent, J. Polym. Sci.: Symp. **48**, 1 (1974).
[14] G. Strobl, *The Physics of Polymers* (Springer, Berlin, 1997).
[15] H. B. Callen, *Thermodynamics and an Introduction to Thermostatics* (John Wiley & Sons, New York, 1985).
[16] R. J. Atkin and N. Fox, *An Introduction to the Theory of Elasticity* (Dover, Mineola, NY, 1980).
[17] M. Baker and J. L. Ericksen, J. Wash. Acad. Sci. **44**, 33 (1954).
[18] B. Dacorogna, Discrete Contin. Dynam. Syst. Ser. B **1**, 257 (2001).
[19] R. G. Larson, *Constitutive Equations for Polymer Melts and Solutions* (Butterworths, Boston, 1988).
[20] Z. Abiza, M. Destrade, and R. W. Ogden, Wave Motion **49**, 364 (2012).
[21] R. S. Rivlin, Philos. Trans. R. Soc. London A **240**, 459 (1948).
[22] M. Mooney, J. Appl. Phys. **11**, 582 (1940).
[23] T. Borg and E. J. Pääkkönen, J. Non-Newton. Fluid Mech. **159**, 17 (2009).
[24] J. D. Huppler, I. F. MacDonald, E. Ashare, T. W. Spriggs, R. B. Bird, and L. A. Holmes, Trans. Soc. Rheol. **11**, 181 (1967).
[25] W. R. Leppard and E. B. Christiansen, AIChE J. **21**, 999 (1975).
[26] J. M. Maerker and W. R. Schowalter, Rheol. Acta **13**, 627 (1974).
[27] A. S. Lodge, *Elastic Liquids* (Academic Press, New York, 1964).
[28] J. Meißner, Pure and Applied Chemistry **56**, 369 (1984).
[29] W. Gleißle, Rheol. Acta **21**, 484 (1982).
[30] H. Pleiner, M. Liu, and H. R. Brand, Rheol. Acta **41**, 375 (2002).
[31] H. Pleiner, M. Liu, and H. R. Brand, in *Modeling of Soft Matter. IMA Volumes in Mathematics and its Applications, Vol. 141: Fluids*, edited by M.-C. T. Calderer and E. M. Terentjev (Springer, New York, 2005), p. 99ff.
[32] D. Collin, G. K. Auernhammer, O. Gavat, P. Martinoty, and H. R. Brand, Macromol. Rapid Commun. **24**, 737 (2003).
[33] Z. Varga, J. Féher, G. Filipcsei, and M. Zrinyi, Macromol. Symp. **200**, 93 (2003).
[34] H. R. Brand and H. Finkelmann, in *Handbook of Liquid Crystals*, edited by J. W. Goodby *et al.* (Wiley, New York, 1998), Vol. 3, p. 277ff.
[35] H. R. Brand, H. Pleiner, and P. Martinoty, Soft Matter **2**, 182 (2006).
[36] K. Urayama, Macromolecules **40**, 2277 (2007).